Structures 46 (2022) 1313–1326

Contents lists available at ScienceDirect

Structures

journal homepage: www.elsevier.com/locate/structures

Structural system identification and damage detection using adaptive hybrid Jaya and differential evolution algorithm with mutation pool strategy

Guangcai Zhang [a], Jiale Hou [a], Chunfeng Wan [a,*], Liyu Xie [b], Songtao Xue [b,c,*]

[a] Key Laboratory of Cncrete and Prestressed Concrete Structure of Ministry of Education, Southeast University, Nanjing, China
[b] Research Institute of Structural Engineering and Disaster Reduction, Tongji University, Shanghai, China
[c] Department of Architecture, Tohoku Institute of Technology, Sendai, Japan

ARTICLE INFO

Keywords:
System identification
Jaya algorithm
Differential evolution
Mutation pool strategy
Sobol sequence
Linear resizing population size

ABSTRACT

Engineering applications of swarm intelligence optimization algorithms have been widely employed to identify structural systems and damages owing to their merits of simplicity, flexibility, robustness etc., while they often suffer from the defects of slow efficiency, premature convergence or even trapping into local optima in solving the inverse problem of nonlinear optimization-based parameter identification with partial noise-contaminated measurements. To deal with this issue, an adaptive hybrid Jaya and differential evolution (AHJDE) algorithm is proposed based on Jaya algorithm and differential evolution (DE) by effectively combining the advantages of both algorithms. In the proposed AHJDE, four improvements including adaptive mutation strategy, dynamic mutation and crossover operators, sampling-based resizing search space and linear resizing population size are integrated. The effectiveness of the proposed method is verified using a numerical example of 20-DOF linear system by comparing its performance with particle swarm optimization, modified artificial bee colony algorithm, clustering tree seeds algorithm, improved butterfly optimization algorithm etc. considering known mass case and unknown mass case. In addition, numerical studies on a nonlinear single degree-of-freedom system with classical Bouc-Wen hysteretic model and improved Bouc-Wen model are implemented to investigate the applicability in the field of nonlinear system identification. Finally, a series of experimental tests on a five-story steel frame structure are conducted in the laboratory to further validate the performance of the proposed approach in damage identification. Identification results demonstrate the proposed AHJDE can accurately and effectively identify the unknown system parameters and damages with limited sensors and noise-polluted responses.

1. Introduction

Continuous health monitoring and early damage identification for the existing and aging infrastructure, such as super high-rise buildings, large-span bridges, concrete dams, underground comprehensive pipe gallery, nuclear power plants, are significantly necessary since the sudden failures of such major civil structures may result in great casualties and property loss. Therefore, in the past few decades, a considerable number of identification methods have been developed and utilized to identify structural parameters and damages, which provides a solid foundation for safety assessment, maintenance arrangement and prediction of future service life, etc.

From the mathematical view, structural system identification can be transformed into an optimization problem in which the objective is to determine the optimal stiffness, mass, damping and other system parameters by minimizing the discrepancy between the estimated responses from the numerical model and the measured responses from the real system. Some comprehensive reviews on the advancement of structural identification methods have been published [1–3], and considerable frequency-domain and time-domain identification methods have been proposed. For frequency-domain methods, various modal properties extracted from the structural dynamic responses, such as natural frequencies [4], mode shapes [5], curvature mode shapes [6], frequency response functions [7], model flexibility [8], were

* Corresponding authors at: Key Laboratory of Concrete and Prestressed Concrete Structure of Ministry of Education, Southeast University, Nanjing, China (C. Wan); Research Institute of Structural Engineering and Disaster Reduction, College of Civil Engineering, Tongji University, Shanghai, China (S. Xue).
E-mail addresses: guangcaizhang@seu.edu.cn (G. Zhang), houseu@seu.edu.cn (J. Hou), wan@seu.edu.cn (C. Wan), liyuxie@tongji.edu.cn (L. Xie), xue@tongji.edu.cn (S. Xue).

https://doi.org/10.1016/j.istruc.2022.10.130
Received 30 September 2022; Received in revised form 28 October 2022; Accepted 28 October 2022

successfully applied into identification of structural parameters especially for the case of absent measurement of input excitations. However, most of these methods are generally unreliable for structural identification due to their inherent drawbacks that local or minor damages of structural elements may not lead to relatively obvious changes in natural frequencies, and the environmental temperature variation possibly causes more changes in frequencies than damage did. Mode shapes are more sensitive to small damages than frequencies, which is beneficial to improve identification accuracy, but high mode shapes are quite difficult to be accurately acquired owing to recorded signals are unavoidably polluted by noise [9].

On the contrary, identification methods in time domain directly use the raw measurements (accelerations, velocities, displacements, strains, etc.) recorded by sensors installed on the structures. Diverse time domain-based approaches including the recursive least-square method [10], the enhanced sensitivity method [11], the maximum likelihood method [12], the particle filter method [13], the extended Kalman filter method [14], the constrained unscented Kalman filter method [15] had been successfully employed. For instance, Lu et al. [16] proposed a time domain sensitivity-based approach to identify breathing crack, and proved its accuracy and effectiveness with three numerical examples. Lei et al. [17] developed a new method of unscented Kalman filter with unknown input to simultaneously identify nonlinear structural parameters and unknown input force. Although most of aforementioned methods are derived from sound mathematic theories, a good initial estimation of the unknown variables and proper gradient information of the objective function are usually required. Besides, these classical methods are prone to be sensitive to noise and trapped into the local optimum because of their point-to-point search strategy. In contrast, non-classical methods, e.g., machine learning techniques and heuristic optimization algorithms have received increasing attention recently owing to their advantages of simplicity, flexibility, robustness and no derivation. Neural network is an important part of machine learning techniques, and its applications in structural identification have been widely reported. Pathirage et al. [18] applied the deep sparse autoencoder to identify the damages of a prestressed concrete bridge in the laboratory. Ding et al. [19] used sparse deep belief network based on arctan to identify damage locations and severities with limited modal data. Neural network-based methods have strong capacities of nonlinear mapping, robustness, self-learning and self-adapting, while numerous training samples and demanding computational time are required to train the network before identification of structural system.

Compared with classical optimization methods, population-based stochastic search algorithms are more robust to solve the high dimensional and complex optimization problems since there are no requirements for the good initial guess of parameters and the behaviors of objective function (monotonicity, derivability, modality). Therefore, swarm intelligence optimization algorithms, such as genetic algorithm (GA) [20], particle swarm optimization (PSO) [21], differential evolution (DE) [22], modified artificial bee colony algorithm (modified ABC) [23], big bang-big crunch optimization algorithm (BB-BC) [24], wolf algorithm [25], teaching–learning-based optimization algorithm (TLBO) [26], water strider algorithm [27], clustering based tree seeds algorithm (C-TSA) [28] have been increasingly developed and employed in recent years. For example, Kaveh et al. [29] applied seven swarm optimization algorithms to optimize plane steel frame structures. Wang et al. [30] utilized four different evolutionary algorithms including gradient search, GA, PSO, hybrid PSO and gradient search to identify structural parameters. Zhou et al. [31] developed an improved butterfly optimization algorithm (IBOA) for structural identification. However, for most of these heuristic algorithms, trial-and-error strategy is generally adopted to select controlling parameters, which inevitably wastes much computing time. Instead, a novel parameter-free swarm intelligence algorithm, named Jaya algorithm, was proposed by Rao to solve constrained or unconstrained optimization problems [32]. Jaya algorithm has reasonable optimization idea that the offspring will move toward the best-so-far solution and meanwhile away from the worst solution. Then, the quality of solutions will be continuously improved. Diverse real-world applications of Jaya algorithm have been presented, such as training neural network [33], controller design of automatic generation control [34], size optimization of truss structures [35], inverse identification of concrete dams [36], structural damage identification [37]. Nevertheless, as an emerging algorithm, Jaya still suffers from the limitations of slow convergence rate and easiness of being trapped into local optimal solution due to its relatively simple mutation mechanism, especially for solving multimodal and multi-dimensional optimization problems.

To improve the performance of Jaya algorithm, some attempts have been made in recent years. For instance, Rao and Saroj [38] proposed a self-adaptive multi-population Jaya algorithm by dividing the population into multiple sub-populations. Yu et al. [39] constructed an improved Jaya algorithm by introducing self-adaptive weight, experience-based learning strategy and chaotic elite learning strategy. Besides introducing new improvement techniques to further explore the merits of Jaya algorithm, hybridizing two or more algorithms simultaneously provides an alternative with the attractive concept of effectively combing individual advantages of different algorithms with following successful applications, such as hybrid bat algorithm and DE [40], hybrid butterfly optimization and DE algorithm [41], etc. Indeed, it is important for a heuristic algorithm to achieve the balance between exploring new regions in the predefined search domain and utilize the existing information. Jaya algorithm has relatively poor global exploration capacity since individuals in the population are guided by the best-so-far solution. Contrary to Jaya, DE has stronger global search ability and more variants of mutation schemes. Thus, Jaya and DE have already been hybridized and reported in some latest published papers, such as hybrid Jaya and DE algorithm [42], hybrid adaptive DE and Jaya algorithm [43], competitive hybrid DE and Jaya algorithm [44], hybrid Jaya algorithm with double coding [45], modified Jaya algorithm [46]. However, these algorithms still experience some issues to be addressed. Only one mutant operator of DE, i.e., DE/rand/1 or DE/rand/2, is hybridized with Jaya mutation, which may limit the performance of hybrid algorithm due to the relatively simple mutation operations. In some existing hybrid schemes, the mutation operations of DE and Jaya are simply implemented in sequence, resulting in more computational resources inevitably consumed. Besides, the scaling factor, crossover operator, population size, search space limits of unknown parameters are usually constants during the searching process, which is unfavorable to computational efficiency and accuracy.

In consideration of these limitations, this paper proposes a novel hybrid algorithm, i.e., adaptive hybrid Jaya and differential evolution (AHJDE) algorithm based on four different improvement techniques to solve structural system identification and damage detection problem. The main contributions of this paper are the suggestion of a powerful AHJDE algorithm. First, an adaptive updating scheme is developed based on mutation pool strategies, namely, DE/rand/1 and DE/rand/2 in exploration group, DE/current-to-best/1 and Jaya mutation in exploitation group. Such an adaptive mutation strategy is beneficial to effectively combine the local exploitation capability of Jaya algorithm and the global exploration capability of DE in different stage. Second, dynamic mutation and crossover operators are introduced to keep the trade-off between the global and local search abilities. Third, a sampling-based resizing search space method is proposed to effectively narrow the search limits of unknown parameters. Fourth, a linear resizing population size technique is applied to continually eliminate some individuals with low quality from the current population to accelerate convergence rate and reduce the risk to be trapped into local optimum. The performance of the proposed AHJDE algorithm in identifying structural parameters and damages with partial noise-polluted acceleration measurements is investigated by not only numerical simulations on the linear and nonlinear systems but also experimental tests on a laboratory-five-story steel frame structure.

2. Problem formulation

Identification of structural models or damages can be treated as an optimization problem solved by optimization algorithms, as shown in Fig. 1. The objective is to find the best parameters $\widehat{\theta}$ by minimizing the discrepancy between the measured structural acceleration responses $\ddot{u}(t_k)$ and the estimated acceleration responses $\widehat{\ddot{u}}\left(\widehat{\theta}, t_k\right)$ as follows

$$obj(\widehat{\theta}) = \sum_{i=1}^{n_{sen}} \sum_{k=1}^{n_{time}} \frac{\left\| \widehat{\ddot{u}}_i(\widehat{\theta}, t_k) - \ddot{u}_i(t_k) \right\|^2}{E\left(\ddot{u}_i^2(t_k)\right)} \tag{1}$$

where $\widehat{\theta} = \left\{ \widehat{\theta_1}, \widehat{\theta_2}, ..., \widehat{\theta_n} \right\}$ denotes system's parameters including unknown structural parameters, stiffness, damping and mass, and nonlinear hysteretic parameters, etc.; n_{sen} and n_{time} stand for the number of measurements and recorded samples, respectively; $\| \cdot \|$ means the Euclidean norm; $E\left(\ddot{u}_i^2(t_k)\right) = \frac{1}{n_{time}} \sum_{k=1}^{n_{time}} \ddot{u}_{mea}^2(t_k)$ represents mean squared value of the i-th response history. Herein, the inverse formation of objective function is employed as the fitness function $fit\left(\widehat{\theta}\right)$

$$fit\left(\widehat{\theta}\right) = \frac{1}{\varepsilon + \text{obj}\left(\widehat{\theta}\right)} \tag{2}$$

where ε is set as a small value to avoid a potential zero denominator. If the estimated system parameters agree well with the actual value, namely$\text{obj}\left(\widehat{\theta}\right) = 0$, the maximum fitness value will be equal toε^{-1}. The solution whose fitness function value is closer to ε^{-1} is better, which is beneficial to obviously reflect the quality of the identified solution. The problem of structural system identification is summarized as follows

$$\begin{aligned} &\text{maximize} \quad fit\left(\widehat{\theta}\right), \widehat{\theta} = \left\{ \widehat{\theta}_1, \widehat{\theta}_2, ..., \widehat{\theta}_n \right\} \\ &s.t. \quad \widehat{\theta} \in \Gamma, \quad \Gamma = \left\{ \widehat{\theta} : \theta_j^{\min} \leqslant \widehat{\theta}_j \leqslant \theta_j^{\max}, \quad \forall j = 1, 2, ..., \text{Dim} \right\} \end{aligned} \tag{3}$$

where Dim is the number of unknown parameters to be identified; Γ means the Dim-dimensional search domain; $\theta_j^{\min}$ and $\theta_j^{\max}$ stand for the lower and upper limits of the j-th parameter.

By Eqs. (1–3), structural system identification can be formulated as a linearly constrained muti-dimensional nonlinear optimization problem, which is a typical inverse problem with limited input and output signals to identify considerable number of unknown parameters. In this case, some traditional optimization approaches may have difficulties in identifying linear and nonlinear structural models due to their weak search capacity and poor robustness to noise. Therefore, it is necessary to develop more powerful swarm intelligence algorithms.

3. Identification algorithms

In this section, the basic Jaya algorithm and differential evolution are introduced, respectively. Subsequently, the adaptive hybrid Jaya and differential evolution algorithm is proposed by effectively combining Jaya and DE.

3.1. Jaya algorithm

Jaya algorithm is a novel population-based stochastic optimization algorithm, proposed by Rao in 2016. A distinctive feature is that Jaya algorithm does not need any algorithm-specific parameters, except two common parameters, i.e., population size and number of iterations. The pseudo-code of Jaya algorithm is presented in Fig. 2. Jaya algorithm can be mainly divided into three phases, i.e., initialization phase, iteration phase and output phase, elaborated as follows.

Initialization phase: Like other popular swarm intelligence algorithms, Jaya algorithm randomly generates an initial population $(x_1, x_2, ..., x_{NP})$ over the entire search domain

$$\begin{aligned} &x_{j,i} = x_{j,i}^L + rand \times \left(x_{j,i}^U - x_{j,i}^L \right), \\ &i = 1, 2, ..., NP; j = 1, 2, ..., Dim \end{aligned} \tag{4}$$

where $x_{j,i}$ represents the j-th variable of the i-th solution; x_j^U and x_j^L stand for the upper and lower limits ofx_j; $rand$ means a random number taken from the range of [0, 1]; NP and Dim denote the size of population and the number of unknown variables, respectively.

Iteration phase: The update operation is inspired by the concept that offspring ought to move towards the optimal solution and meanwhile escape from the inferior solution. The new solution v_i for the i-th individual x_i is generated by following equation

$$v_{j,i,G} = x_{j,i,G} + rand_1 \times \left(x_{j,best,G} - \left| x_{j,i,G} \right| \right) - rand_2 \times \left(x_{j,worst,G} - \left| x_{j,i,G} \right| \right) \tag{5}$$

where $\left| x_{j,i,G} \right|$ represents the absolute value of$x_{j,i,G}$; $x_{j,best,G}$ and $x_{j,worst,G}$ stand for the value of the j-th variable for the best solution and the worst one at the G-th iteration, respectively; $rand_1$ and $rand_2$ mean two different random numbers in the range of [0, 1]. The second item in Eq. (5) $rand_1 \times \left(x_{j,best,G} - \left| x_{j,i,G} \right| \right)$ denotes the tendency of the new solution to approach the best solution, while the third item $rand_2 \times \left(x_{j,worst,G} - \left| x_{j,i,G} \right| \right)$ shows a trend to escape from the worst solution.

Then, greedy selection mechanism is conducted to determine the original individual x_i or updated solution v_i will survive to the next iteration by comparing their fitness value as follows

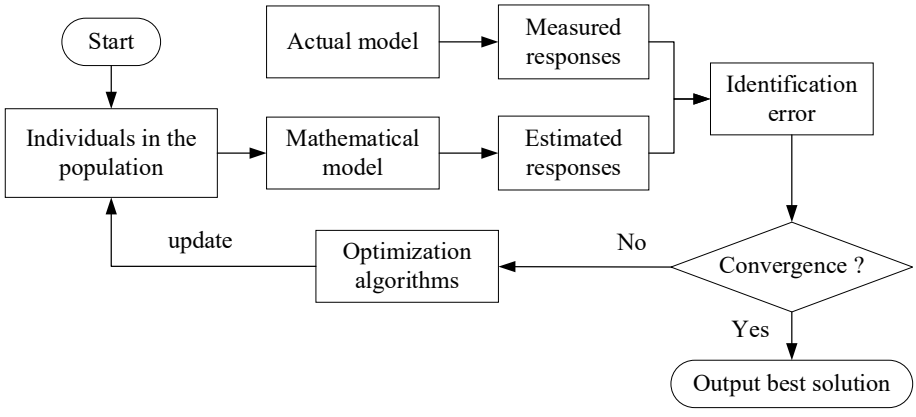

Fig. 1. The process of structural system identification using optimization algorithms.

```
Initialization phase
  Define the population size NP, number of parameters to be identified Dim, termination criterion, maximum
  iterations number Max_Iter
  Randomly generate an initial population with Eq. (4)
  Define fitness function fit
Iteration phase
  Initialize iteration number G = 1
  While termination criterion is not reached do
    Evaluate the fitness value for all individuals in the population
    Sort fitness values and determine the best individual x_{best,G} and the worst one x_{worst,G}
    For individual i = 1 to NP do
      Produce two random number rand_1 and rand_2 uniformly distributed over the interval [0, 1]
      Update solution x_{i,G} using Eq. (5)
    End for
    Evaluate the fitness value of the new updated solution v_{i,G}
    Greedy selection strategy to keep better solution with Eq. (6)
    G = G + 1
  End while
Output phase
    Output the identified best solution and its optimal value
```

Fig. 2. The pseudo-code of Jaya algorithm.

$$x_{i,G+1} = \begin{cases} v_{i,G} \ if \ fit(v_{i,G}) < fit(x_{i,G}) \\ x_{i,G} \ otherwise \end{cases} \tag{6}$$

where $fit(x_{i,G})$ and $fit(v_{i,G})$ denote the fitness function values of x_i and v_i at the G-th iteration. From Eq. (6), solution with better fitness value will be selected for the $(G + 1)$ iteration.

Output phase: The iteration phase will be continually performed until the convergence criterion is satisfied or the predefined maximum iteration number is reached. Finally, the identified best solution and its optimal value are obtained.

3.2. Differential evolution

Differential evolution (DE) is a popular swarm intelligence algorithm, first proposed by Storn and Price to solve real parameter optimization problem [47]. DE has been widely applied into various fields owing to its advantages of simple structure, easy implementation, fast convergence, strong robustness. In DE, search direction is guided by the cooperation and competition among individuals in the population. There are four main procedures of DE, i.e., initialization, mutation, crossover, and selection, roughly described as follows.

Initialization: The initial population $(x_1, x_2, ..., x_{NP})$ is randomly generated within the search bounds $\left[x_j^L, x_j^U\right]$ using Eq. (4). Each individual is considered as a possible solution.

Mutation: Individual variation is realized by differential strategy, which is an effective way to produce new feasible solutions. In the basic mutation operation DE/best/1 of DE, two different individuals $x_{r_2^i,G}$ and $x_{r_3^i,G}$ are randomly chosen from current population. Then, individuals generate a difference vector by subtracting each other, multiply a mutation operator F and add to a third individual vector$x_{r_1^i,G}$. Herein, several commonly referred mutation strategies are listed as below [48]

$$DE/rand/1 : v_{i,G} = x_{r_1^i,G} + F\left(x_{r_2^i,G} - x_{r_3^i,G}\right) \tag{7}$$

$$DE/best/1 : v_{i,G} = x_{best,G} + F\left(x_{r_1^i,G} - x_{r_2^i,G}\right) \tag{8}$$

$$DE/rand/2 : v_{i,G} = x_{r_1^i,G} + F\left(x_{r_2^i,G} - x_{r_3^i,G} + x_{r_4^i,G} - x_{r_5^i,G}\right) \tag{9}$$

$$DE/best/2 : v_{i,G} = x_{best,G} + F\left(x_{r_1^i,G} - x_{r_2^i,G} + x_{r_3^i,G} - x_{r_4^i,G}\right) \tag{10}$$

$$DE/current-to-rand/1 : u_{i,G} = x_{i,G} + F\left(x_{r_1^i,G} - x_{i,G} + x_{r_2^i,G} - x_{r_3^i,G}\right) \tag{11}$$

$$DE/current-to-best/1 : v_{i,G} = x_{i,G} + F\left(x_{best,G} - x_{i,G} + x_{r_1^i,G} - x_{r_2^i,G}\right) \tag{12}$$

where $x_{i,G}$, $v_{i,G}$ and $u_{i,G}$ stand for the target individual, mutant individual and trial individual, respectively; r_1^i, r_2^i, r_3^i, r_4^i and r_5^i are mutually different integers randomly chosen from the range of [1, NP], and they are also different from the base index i, namely $r_1 \neq r_2 \neq r_3 \neq r_4 \neq r_5 \neq i$; $x_{best,G}$ means the identified best-so-far solution with the maximum fitness value at the G-th iteration; F represents mutation operator generally taken from the range of [0, 1], which scales the amplification of the differential vectors. It is noted that DE/current-to-rand/1 does not involve a binomial crossover.

Crossover: Binomial crossover operation is implemented to improve the diversity of the population following the mutation operation. The mutated individual $v_{i,G}$ mixes its components with the original target individual $x_{i,G}$ to generate a trial individual$u_{i,G}$. If a randomly produced number within the range [0, 1] is less than predefined crossover operatorCR, binomial crossover will be performed as follows

$$u_{j,i,G} = \begin{cases} v_{j,i,G} & if\left(rand_j[0, \ 1] \leqslant CR\right) or (j = j_{rand}), j = 1, 2, ..., Dim \\ x_{j,i,G} & otherwise \end{cases} \tag{13}$$

where CR is crossover operator; $rand_j[0, \ 1]$ denotes a random number within the range [0, 1]; j_{rand} means a random integer from [1, Dim] to ensure trial individual $u_{i,G}$ and $x_{i,G}$ are different.

Selection: Selection operation is performed to make the better solution between the target (parent) individual $x_{i,G}$ and the trial (offspring) individual $u_{i,G}$ survive to the next iteration as described in Eq. (6).

Mutation, crossover, selection operations are repeated until convergence criterion or number of maximum iterations are satisfied. Taking the mutation strategy of DE/best/1 as example, the pseudo-code of DE is shown in Fig. 3.

3.3. Adaptive hybrid Jaya and differential evolution algorithm

To improve the performance of Jaya algorithm, an adaptive hybrid Jaya and DE algorithm is proposed by introducing adaptive mutation strategy, dynamic mutation and crossover operators, sampling-based resizing search space, linear resizing population size.

3.3.1. Adaptive mutation strategy

It is necessary for swarm intelligence algorithms to focus on different tasks in different stages. More specifically, a powerful exploration capacity is desired to take any promising solution into consideration in the early stage. As the population evolves, a strong exploitation capacity is

Set the size of population *NP*, dimension of variables to be identified *Dim*, initial mutation operator *F*, initial crossover operator *CR*, termination criterion, maximum iterations number *Max_Iter*
Randomly generate an initial population with Eq. (4)
Define and evaluate the fitness value for each individual
Initialize iteration number $G = 1$
While termination criterion is not reached **do**
  For individual $i = 1$ to *NP* **do**
    Randomly select three different individuals satisfying $r_1 \neq r_2 \neq r_3 \neq i$
    Generate the mutant individual $v_{i,G}$ with Eq. (7)
    Generate the trial individual $u_{i,G}$ with Eq. (13)
    Ensure all solutions in the population within the upper and lower bounds
    Evaluate the fitness value for each trial individual
    Choose better solution with greedy selection strategy using Eq. (6)
  End for
  $G = G + 1$
End while
Output the best solution and optimal value

Fig. 3. The pseudo-code of DE.

expected to quickly refine the quality of the best solution. An adaptive updating scheme is proposed based on the strategies of mutation pool, which has two different groups, i.e., the exploration group $Group_1$ and the exploitation group$Group_2$, expressed as Eqs. (14) and (15), respectively

$$Group_1 = \begin{cases} v_{i,G} = x_{r_1^i,G} + F\left(x_{r_2^i,G} - x_{r_3^i,G}\right), \ if\ rand(0,1)<0.5 \\ v_{i,G} = x_{r_1^i,G} + F\left(x_{r_2^i,G} - x_{r_3^i,G} + x_{r_4^i,G} - x_{r_5^i,G}\right), \ otherwise \end{cases} \tag{14}$$

where $Group_1$ consists of two mutation strategies of DE/rand/1 and DE/rand/2 with strong exploration capability; rand$(0,1)$ means a random number taken from the range of [0, 1].

$$Group_2 = \begin{cases} v_{i,G} = x_{i,G} + F\left(x_{best,G} - x_{i,G} + x_{r_1^i,G} - x_{r_2^i,G}\right), if rand(0,1)<0.5 \\ \text{Jaya mutation}, \ otherwise \end{cases} \tag{15}$$

where $Group_2$ has two different mutation strategies of DE/current-to-best/1 and Jaya mutation with powerful exploitation capacity.

Different mutation strategies are selected by adjusting the proportion of exploration or exploitation groups, which can be stated as follows

$$\text{Mutation pool} = \begin{cases} \text{Select one strategy from } Group_1, if\ rand(0,1) > \dfrac{Iter}{Max\_Iter} \\ \text{Select one strategy from } Group_2, otherwise \end{cases} \tag{16}$$

where *Iter* indicates the number of consumed iterations; *Max_Iter* means the total number of iterations when the computation is terminated.

It is noted from Eq. (16) that mutation strategies in $Group_1$ and $Group_2$ are selected with higher probability in the early stage and in the later evolution stage, respectively. $Group_1$ has favorable global exploration capacity while $Group_2$ features outstanding local exploitation capacity. In this regard, the global and local search ability can be guaranteed.

3.3.2. Adaptive operators

The optimization performance of DE is affected by mutation operator *F* and crossover operator *CR*. To avoid unpleasant results owing to manually selecting improper parameters, dynamic operators are proposed and utilized.

Adaptive mutation operator *F* varied with the iteration number is expressed as

$$F = F_0 \times 2^{\mu}, \qquad \mu = e^{1 - \frac{Max\_Iter}{Max\_Iter + 1 - Iter}} \tag{17}$$

where F_0 is a constant, whose value is set as 0.4. *F* is equal to maximum value 0.8 at the first iteration, which is conductive to achieve diversity of seeking directions to alleviate the probability of premature convergence. Then, mutation operator *F* gradually decreases as the iteration number increases, which is beneficial for converging to the best optimum.

Unlike a fixed value in original DE algorithm, adaptive crossover operator *CR* of mutation individual v_i is developed associated with its fitness value as follows

$$CR_i = CR_{max} + (CR_{max} - CR_{min}) \times \frac{f_{min} - f_i}{f_{max} - f_{min}} \tag{18}$$

where CR_{min} and CR_{max} stand for the minimum and maximum values of crossover operator,$CR_{min} = 0.3$, $CR_{max} = 0.8$; f_{min} and f_{max} indicate the fitness values of the worst and best individuals in the current population, respectively. By Eq. (18), each mutation solution v_i has its corresponding crossover operator CR_i within the range of$[CR_{min}, CR_{max}]$. Large values of *CR* are obtained for mutant individuals with bad fitness, which decreases their possibility of being restored to the next iteration. On the contrary, small values of *CR* are adopted for mutant individuals with good fitness, which increases their possibility of surviving to the next iteration. Compared with fixed value, adaptive operator is beneficial to reserve better mutant individuals and remove worse ones.

3.3.3. Sampling-based resizing search space

Swarm intelligence algorithms may suffer from slow convergence rate and premature convergence if given a relatively large search space, especially for the complex multi-peak optimization problems. Obviously, reducing initial search limits can improve identification accuracy and efficiency. Accordingly, a sampling-based resizing search space method is proposed to effectively narrow the boundaries of variables and meanwhile without missing the global optimum.

Sampling methods, such as Latin hypercube sampling, Halton sequences, Faure sequences, Niederreiter sequences, can roughly represent and infer the information of fitness surface by implementing small-scale sampling tests. Herein, a popular low-discrepancy sequence, Sobol sequences, is employed to generate quasi-random sequences with the uniform space-filling properties for exploring the multi-dimensional solution domain. Compared with traditional pseudo-random sequences, Sobol sequences can sample *Dim*-dimensional search spaces more evenly. Nowadays, Sobol sequences have been widely utilized in computational finance [49], initialization of heuristic algorithm [50], sensitivity analysis [51], etc.

Sobol sequences are generated based on a set of 'direction numbers'$\lambda_1, \lambda_2 \cdots$, which can be defined as$\lambda_i = \frac{m_i}{2^i}$. m_i is the odd positive integer, less than2^i. To obtain direction numbersλ_i, a primitive polynomial of degree *p* is introduced, written as following form

$$\psi(d) = d^p + c_1 d^{p-1} + \cdots + c_{p-1} d + d^0 \tag{19}$$

where coefficients $(c_1, c_2, \ldots, c_{p-1})$ of primitive polynomial $\psi(d)$ take the value of either 0 or 1.

Then, coefficients of polynomial are used to calculate λ_i by the recurrence relation

$$\lambda_i = c_1\lambda_{i-1} \oplus c_2\lambda_{i-2} \oplus \cdots \oplus c_{p-1}\lambda_{i-p+1} \oplus \lambda_{i-p} \oplus \left(\lambda_{i-p} * 2^{-p}\right), i > p \tag{20}$$

where $\oplus$ stands for a bit-by-bit exclusive-or operation.

Antonov and Saleev proposed Gray code to improve the efficiency of generating Sobol sequences [52]. The i-th number in the Sobol sequences is formed by

$$S_i = g_1\lambda_1 \oplus g_2\lambda_2 \oplus \cdots \tag{21}$$

where $\ldots g_3 g_2 g_1$ is the Gray code representation of i.

In the proposed sampling-based resizing search space method, new boundaries of each variable are resized by the minimum and maximum values of the first Nb samples with better fitness values in the Sobol sequences. The search space limits of variables confined by the selected samples can be expressed as

$$\Gamma = \{[LB_1, UB_1], [LB_2, UB_2], \ldots, [LB_{Dim}, UB_{Dim}]\} \tag{22}$$

where LB_i and UB_i stand for the lower and upper limits of the i-th variable over the selected Nb samples, respectively; Dim means the dimension of unknown parameters to be identified.

Number of the first Nb best samples is computed by $Nb = \delta \times samp\_size$. δ is a selecting fraction and it determines the number of selected samples. $samp\_size$ denotes total sample size. The value of δ should be properly set because it has significant effect on the performance of the proposed method [53].

3.3.4. Linear resizing population size

Population size of swarm intelligence optimization algorithms has significant effect on their performance. On the one hand, small population size is conducive to convergence speed but increases the risk of being trapped into the local optimum. On the other hand, a large population size is beneficial for widely exploring search space but suffers from the disadvantage of slow convergence rate. Therefore, instead of setting a fixed value for population size NP, a linear resizing population size technique is employed to continually decreases the size of population in accordance with a deterministic linear function [54]. The population size NP_{G+1} in the $(G+1)$ iteration can be calculated according to the following equation

$$NP_{G+1} = round\left[\left(\frac{NP_{min} - NP_{init}}{Max\_Iter}\right) \times Iter + NP_{init}\right] \tag{23}$$

where NP_{init} represents the initial population size when iteration number is 1; NP_{min} stand for the population size at the end of iterations, which is associated with the smallest number of individuals so that mutation operation of AHJDE algorithm can be implemented. The $(NP_G - NP_{G+1})$ worst-ranking solutions with unfavorable fitness value will be eliminated from the current population whenever $NP_G > NP_{G+1}$.

3.3.5. Framework of AHJDE

In the proposed AHJDE algorithm, four improvements including adaptive mutation strategy, adaptive mutation and crossover operators, sampling-based resizing search space and linear resizing population size are introduced. The detailed pseudocode of the proposed AHJDE algorithm is presented in Fig. 4. During the implementation of AHJDE, Sobol sequences sampling method is first used to take small-scale samples and resize the initial large search space by the minimum and maximum values of the first Nb best samples. A linear resizing population size technique is utilized to continually eliminate the worst-ranking individuals from the current population with the purpose of accelerating convergence speed and improving identification accuracy. A self-adaptive updating scheme is proposed based on mutation pool strategies, i.e., DE/rand/1 and DE/rand/2 in $Group_1$, DE/current-to-best/1 and Jaya mutation in $Group_2$, to achieve exploration or exploitation in different stages. Adaptive mutation and crossover operators are developed to further improve the performance of hybrid algorithm. It can be observed from Fig. 4 that multiple mutation strategies are combined in the proposed AHJDE algorithm, which can effectively modify the original Jaya algorithm and meanwhile not obviously increase the fitness function evaluations.

```
Define the population size NP_init and NP_min, number of parameters to be identified Dim, termination criterion,
maximum iterations number Max_Iter, initial mutation operator F and crossover operator CR
Generate samples with Sobol sequences to resize the search space
Randomly generate an initial population within the confined search space
Initialize iteration number Iter = 1
While termination criterion is not reached do
  Linear resizing population size with Eq. (23)
  Define and evaluate the fitness value for each candidate
  Sort fitness values and determine the best individual and the worst one
  For individual i = 1 to NP do
    If rand(0,1) > Iter/ Max_Iter
      If rand(0,1) < 0.5
        Update solution using DE/rand/1
      Else
        Update solution using DE/rand/2
      End if
      Implement crossover operation with Eq. (13)
    Else
      If rand(0,1) < 0.5
        Update solution using DE/current-to-best/1
        Implement crossover operation with Eq. (13)
      Else
        Update solution using Jaya mutation
      End if
    End if
  End for
  Update adaptive mutation operator F and crossover operator CR
  Greedy selection strategy to keep better solution
  Iter = Iter + 1
End while
Output the identified best solution and its optimal value
```

Fig. 4. The pseudocode of the proposed AHJDE.

4. Numerical studies

To investigate the performance of the proposed AHJDE algorithm for structural system identification, two numerical studies on a 20-DOF linear system and a SDOF nonlinear system are employed. All numerical analyses are conducted by MATLAB version 2018a on Intel(R) Core i5-11320 CPU @ 3.20 GHz and 16.00 GB of RAM.

4.1. Identification of 20-DOF linear system

As shown in Fig. 5, a two-dimensional shear-type frame structure is modelled as *n*-DOF linear structural system. The dynamic equation of motion for this system can be expressed as

$$M\ddot{u}(t) + C\dot{u}(t) + Ku(t) = f(t) \tag{24}$$

where M, C, and K stand for mass, damping and stiffness matrices, respectively;$u(t)$, $\dot{u}$(t) and $\ddot{u}(t)$ are displacement, velocity, acceleration vectors, respectively; $f(t)$ represents the time-dependent input force vector. The Rayleigh damping matrix C is calculated by a linear combination of the stiffness matrix K and the mass matrix M

$$C = aM + bK, \qquad \zeta_r = \frac{a}{2\omega_r} + \frac{b\omega_r}{2} \tag{25}$$

where a and b are unknown constant damping coefficients. 5 % modal damping ratio ζ_r is set in the first two modes of vibration ($r = 1$ and 2). ω_r means the r-th natural frequency. Structural dynamic responses are simulated by the Newmark's constant-average-acceleration method.

A 20-DOF linear system is selected as numerical example to validate the applicability of the proposed AHJDE algorithm to structural system identification, which had been utilized in Refs. [22] and [55]. Structural properties of the 20-DOF system are given in Table 1. Both the known and unknown mass case are considered. Two physical quantities, stiffness and modal damping ratios, are assumed as unknown parameters to be identified for known mass case. While three physical quantities, stiffness, mass, modal damping ratios, are assumed as unknown parameters for unknown mass case. As presented in Fig. 5, input forces are applied to the 20-DOF structure at every 5th level in the horizontal direction as Gaussian noise sequences with the RMS of the force scaled to 1000 N. For known mass case, acceleration responses with sampling rate of 1000 samples/s and total duration of 2 s, are recorded by 8 accelerometers, located at the 2nd, 4th, 7th, 10th, 12th, 14th, 17th, 20th floors.

Table 1
The structural properties of 20-DOF system.

Parameters	Numbers	Value
Stiffness (kN/m)	Levels 1–10	5000
	Levels 11–15	4000
	Levels 16–20	3500
Mass (kg)	Levels 1–10	4000
	Levels 11–20	3000
Natural period of vibration (s)	First mode	2.123
	Second mode	0.797

While 12 accelerometers were installed at the 1st, 2nd, 3rd, 4th, 6th, 8th, 10th, 12th, 14th, 16th, 18th, 20th floors for the unknown mass case, considering its rather more complexity of the system. The search space limits for each parameter are set as half to twice their corresponding exact value.

4.1.1. Known-mass linear system

There are 22 unknown parameters to be identified for the 20-DOF known mass case. The parameters of the proposed AHJDE method are population sizes$NP = 100$, maximum iterations number$Max_Iter = 300$, samples size$samp_size = 400$, selecting fraction $\delta = 0.1$, $Nb = 40$. ε is set as 0.001, so the maximum fitness value is equal to 1000. The average results based on 20 independent runs with AHJDE are listed in Table 2 and compared with those obtained by mature and state-of-the-art algorithms, i.e., SSRM [55], PSO [22], DE [22], modified ABC [23], C-TSA [28], IBOA [31]. It can be observed that the proposed AHJDE provides the most satisfactory results among seven

Table 2
Mean and maximum errors for 20-DOF known mass system without noise (%).

Results	SSRM[a]	PSO[b]	DE[b]	Modified ABC[c]	C-TSA	IBOA	AHJDE
Mean error-K	0.52	0.71	0.41	0.19	0.33	0.17	0.01
Max error-K	1.60	3.37	1.29	1.04	1.28	1.08	0.04
Mean error-C	0.64	2.24	0.53	0.19	1.01	1.30	0.16
Max error-C	1.21	8.31	1.45	1.06	2.78	1.75	0. 68

Note: [abc]Results obtained from Refs. [55], [22] and [23], respectively.

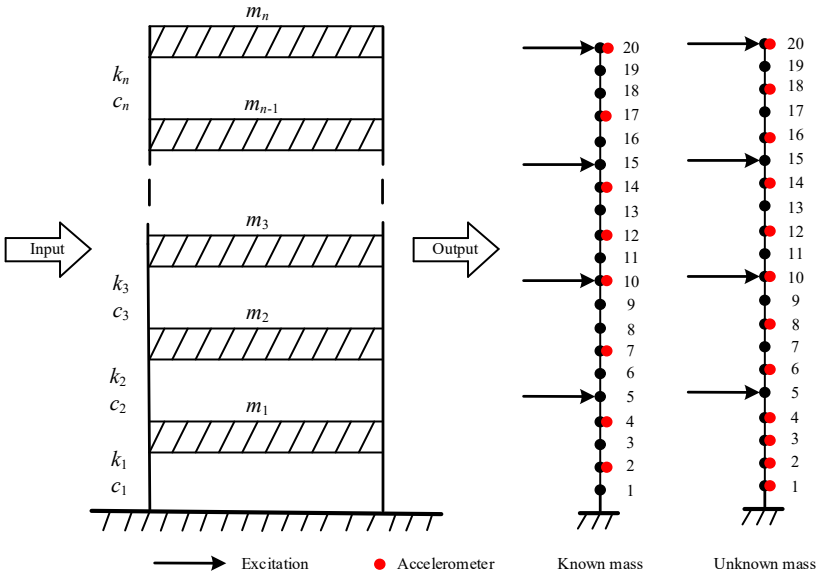

Fig. 5. Numerical model of 20-DOF structure.

identification methods with the minor maximum errors of only 0.04 % and 0.68 % in the identification of stiffness and damping parameters, respectively. Fig. 6 shows the fitness value and mean error of 20-DOF known mass system by the proposed AHJDE, and Fig. 7 presents the convergence histories of estimated stiffness without noise corruption. Obviously, identified stiffness parameters of all elements converge to their corresponding actual values, namely element stiffness K_1-K_{10} = 5000 kN/m, K_{11}-K_{15} = 4000 kN/m, K_{16}-K_{20} = 3500 kN/m. By Fig. 6, the fitness value approximates its maximum value 1000 after 200 iterations, which indicates the proposed AHJDE algorithm can accurately and effectively identify stiffness and damping parameters for known mass system.

To investigate the robustness of proposed AHJDE to measurement noise in identifying structural parameters, white Gaussian noise sequences are introduced into the clean measurements $\ddot{u}_{\text{clean}}$

$$\ddot{u}_{mea} = \ddot{u}_{clean} + noise = \ddot{u}_{clean} + Nl \times N_{noise} RMS\left(\ddot{u}_{clean}\right) \tag{26}$$

where $\ddot{u}_{\text{mea}}$ represents the measured signals; Nl means the level of noise, and 5 % and 10 % noise levels are considered; N_{noise} denotes the noise vector of Gaussian distribution with zero mean and unit standard deviation; $\text{RMS}\left(\ddot{u}_{\text{clean}}\right)$ stands for the root-mean-square of the recorded acceleration. The identified results of stiffness based on 20 independent runs by Jaya, C-TSA, IBOA and AHJDE are presented in Fig. 8. Among these four methods, Jaya provides the worst identification results with more than 7 % maximum error under 5 % noise. Better performance is acquired by C-TSA and IBOA, but more than 2 % mean error and 5.5 % maximum error are still not accurate enough. In contrast, the proposed AHJDE method provides the most excellent parameter estimation with mean error and maximum error less than 1.1 % and 2.5 % for the worst 10 % noise case, which demonstrates AHJDE algorithm is accurate and robust to identify structural unknown parameters.

4.1.2. Unknown-mass linear system

There are 42 unknown parameters to be identified for the 20-DOF unknown mass case. The parameters of the proposed AHJDE method are population sizesNP = 200, maximum iterations numberMax_Iter = 400, samples size$samp_size$ = 600, selecting fraction $\delta = 0.1$, $Nb = 60$. For noise free case, the identified results for 20-DOF unknown mass system are displayed in Fig. 9. Small identification errors are obtained by AHJDE with the maximum error 0.72 % for stiffness and 1.03 % for mass parameters. When 5 % and 10 % noise are considered, the identified results of AHJDE are summarized in Table 3 and compared with SSRM, PSO, DE, modified ABC, C-TSA, IBOA. The

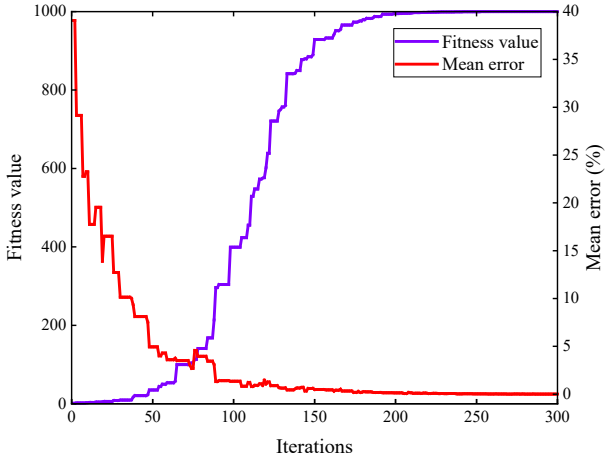

Fig. 6. Fitness value and mean error of 20-DOF known mass system by proposed AHJDE.

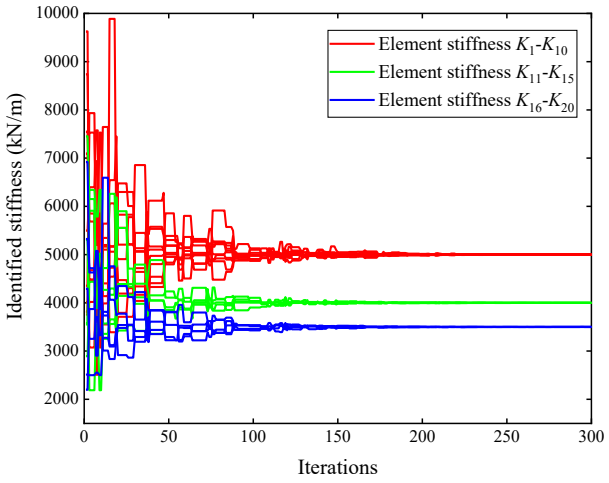

Fig. 7. Convergence results for 20-DOF known mass system with noise-free responses.

convergence histories of stiffness, mass and damping ratios with 10 % noise-contaminated responses are presented in Fig. 10. It can be found that the proposed AHJDE algorithm can provide much better identification results than other six methods with the mean errors of 1.23 % and maximum of 3.62 % in stiffness, and mean error of 1.45 % and maximum of 4.40 % in mass even under 10 % noise. In addition, the evolution process of stiffness, mass, damping ratios indicates that AHJDE algorithm is able to accurately identify parameters of unknown mass system due to its good global and local optimization capacities. The obtained identifications are worse than the previous case owing to the coupling effect of stiffness and mass. Relatively obvious deviation of damping ratios from their actual value are observed in Fig. 10(c), but it is still acceptable with 7.4 % errors for ζ_2 since damping parameters have a relatively small contribution to the structural responses, rendering it difficult to be accurately identified.

Besides, the computational efficiency for these seven identification methods, i.e., SSRM, PSO, DE, modified ABC, C-TSA, IBOA, AHJDE, is further investigated. It is noted that fitness function evaluations for each candidate solution are the main time-consuming operation in the identification process, which is related to solving the second-order ordinary differential equations of motion. Accordingly, the computational efficiency of different identification algorithms can be roughly determined based on the number of evaluations of the fitness function assuming under the same computational condition. By Table 4, the smallest number of 41,903 fitness function evaluations are required for the proposed AHJDE owing to the operation of linear resizing search space, which indicates it can achieve higher computational efficiency than SSRM, PSO, DE, modified ABC, C-TSA, IBOA.

In summary, the strong exploration capability of DE and powerful exploitation capability of Jaya algorithm are effectively combined with mutation pool strategy. Among the above seven methods, the proposed AHJDE needs the least evaluation times but presents the best results in structural system identification.

4.2. Identification of nonlinear SDOF system

Given the excellent performance in the parameters identification of linear structures, AHJDE is applied to the more complex and difficult nonlinear system identification. Numerical studies on a nonlinear SDOF system with classical Bouc-Wen hysteretic model and improved Bouc-Wen model are conducted to verify the effectiveness of the proposed method.

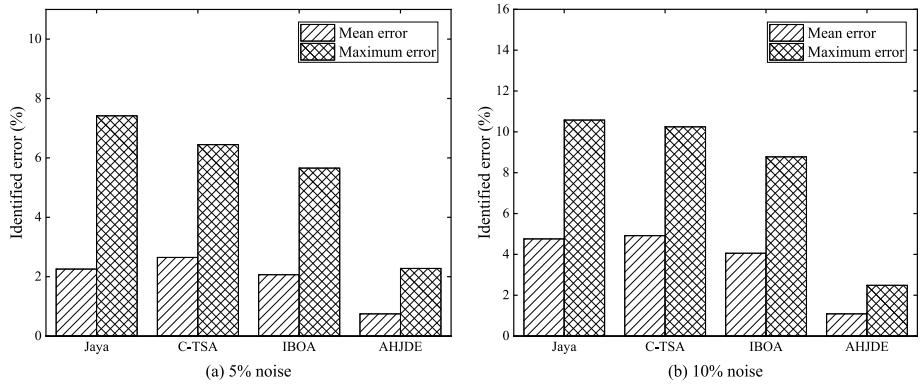

Fig. 8. Results of identified stiffness for known mass system with: (a) 5% noise; (b) 10% noise.

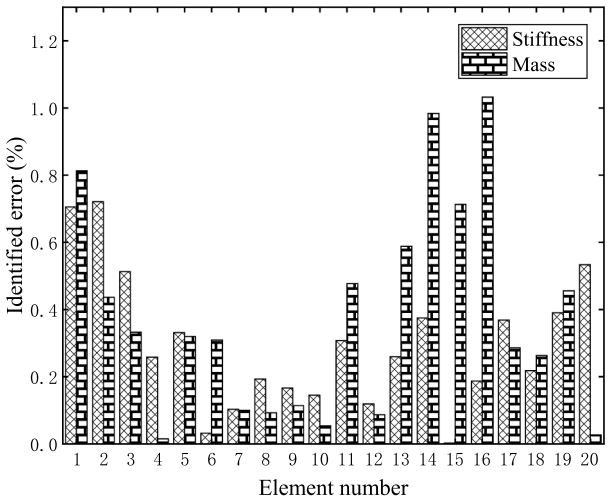

Fig. 9. Identification results of 20-DOF unknown mass system without noise corruption.

4.2.1. Classical Bouc-Wen model

A numerical example of nonlinear SDOF system with hysteretic model is shown in Fig. 11, and its properties are mass $M = 200$ kg, stiffness $K = 7200$ N/m, damping $C = 120$ Ns/m. The Kobe (1995) earthquake record with peak ground acceleration of 3 g is used as input to excite the SDOF system with the sampling frequency of 50 Hz and the duration of 40 s.

The equation of motion for the nonlinear SDOF system can be expressed as

$$M\ddot{u} + C\dot{u} + \mathrm{R}(u,z) = -MI\ddot{g} \tag{27}$$

where $\ddot{g}$ means the earthquake acceleration; $\mathrm{R}(u,z)$ denotes the nonlinear restoring force as written as

$$\mathrm{R}(u,z) = \alpha Ku + (1-\alpha)Kz \tag{28}$$

where α stands for the ratio of post-yield to pre-yield stiffness,$0 \leqslant \alpha \leqslant 1$; z represents the hysteretic displacement. The equation of classical Bouc-Wen model was given by Wen [56] as follows

$$\dot{z} = A\dot{u} - \beta|\dot{u}||z|^{n-1}z - \gamma\dot{u}|z|^{n} \tag{29}$$

where A, β, γ, n are the parameters determining the behavior of the hysteretic model. A is the redundant parameter according to the authors in Ma et al. [57]. More descriptions on the Bouc-Wen model can be

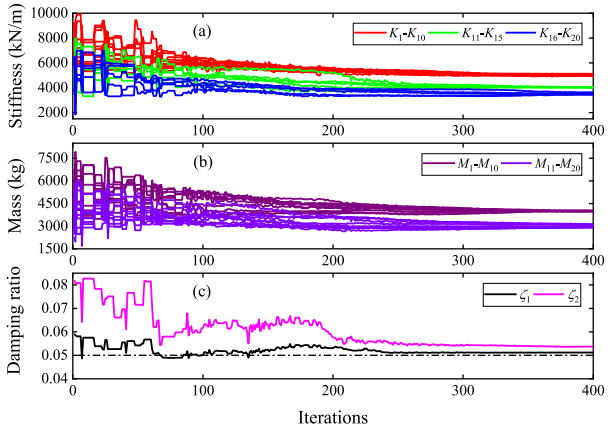

Fig. 10. Convergence histories for 20-DOF unknown mass system with 10% noise: (a) stiffness; (b) mass; (c) damping ratios.

Table 3
Identified errors for 20-DOF unknown mass system under 5% and 10% noise (%).

Noise level	Error	SSRM[a]	PSO[b]	DE[b]	ABC[c]	C-TSA	IBOA	AHJDE
5 %	Mean-K	1.38	3.65	1.27	2.27	1.64	1.21	0.87
	Max-K	3.83	8.13	4.11	5.48	4.52	5.03	3.06
	Mean-M	1.51	3.61	1.42	2.31	2.01	1.88	1.18
	Max-M	4.02	10.81	3.56	5.16	5.46	4.62	3.57
	Mean-C	6.70	10.34	7.23	1.93	2.49	3.13	2.08
	Max-C	12.90	16.57	10.68	5.41	8.75	8.59	5.46
10 %	Mean-K	2.78	5.31	2.63	4.58	2.96	2.76	1.23
	Max-K	8.64	14.36	9.02	11.69	8.78	9.49	3.62
	Mean-M	3.00	7.06	3.29	3.95	3.65	3.84	1.45
	Max-M	10.40	16.27	11.21	9.72	10.22	10.47	4.40
	Mean-C	14.69	17.31	13.54	3.83	4.54	5.42	2.97
	Max-C	20.36	29.06	21.04	12.26	13.95	12.51	8.62

Note: [abc]Results obtained from Refs. [55], [22] and [23], respectively.

Table 4
Comparison of computational efficiency for 20-DOF unknown mass system.

Methods	Initial population size	Iterations	Total evaluations
SSRM[a]	270	7410	2,000,700
PSO[b]	400	500	200,000
DE[b]	400	500	200,000
Modified ABC[c]	180	500	95,095
C-TSA	200	400	80,000
IBOA	200	400	80,000
AHJDE	200	400	41,903

Note: [abc]Results obtained from Refs. [55], [22] and [23], respectively.

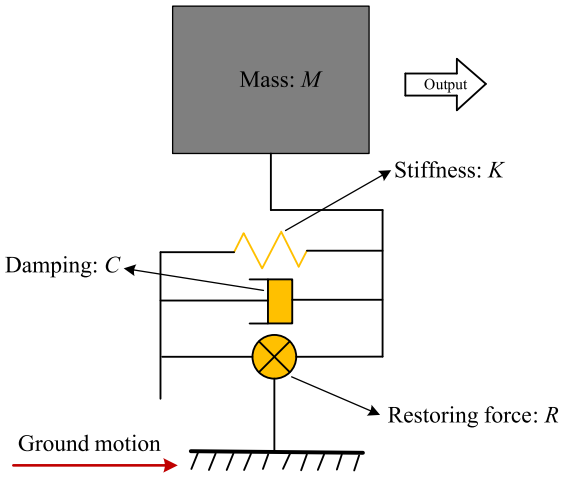

Fig. 11. A nonlinear SDOF system with Bouc-Wen hysteretic model.

found in Ref. [56]. Herein, $\beta = 5$, $\gamma = 5$, $n = 1$ are set. The Eqs. (27–29) are written in state-space form as follows

$$\begin{cases} \dot{u} = y \\ \dot{y} = -\ddot{g} - M^{-1}[\alpha K u + (1-\alpha)Kz + Cy] \\ \dot{z} = y\{1 - [\beta sgn(yz) + \gamma]|z|^n\} \end{cases} \tag{30}$$

where $sgn(\cdot)$ means the signum function. Eq. (30) can be solved by the fourth to fifth order embedded Runge-Kutta integration method.

The common parameters of Jaya, DE and AHJDE are defined as population sizes $NP = 100$, maximum iterations number $Max\_Iter = 200$. Mutation operator $F = 0.8$ and crossover operator $CR = 0.85$ are set for DE, and samples size is set as 300 for AHJDE. Six parameters of nonlinear SDOF system to be identified are stiffness, damping and nonlinear hysteresis parameters, $\widehat{\theta} = \{K, C, \alpha, \beta, \gamma, n\}$. Mass parameters are assumed to be known in prior. The identified results with 0 % and 5 % noise-contaminated acceleration responses are listed in Table 5. It can be seen that the proposed AHJDE is able to provide much more accurate identification results than Jaya and DE. The maximum error obtained by AHJDE ranges from 2.0 % to 5.0 % in the noise free and noise polluted cases, while the corresponding error ranges from 8.9 % to 11.5 % for Jaya algorithm and from 6.3 % to 9.6 % for DE. Furthermore, Fig. 12 presents the hysteretic loops of the classical Bouc-Wen model with AHJDE method. It is observed that the identified hysteretic loop has good agreement with the original curves, and the parameter identification still can be achieved by the proposed approach even if the simulated responses are polluted by 5 % noise, which proves the effectiveness of AHJDE in the identification of nonlinear system.

4.2.2. Improved Bouc-Wen model

Over the years, the classical Bouc–Wen hysteretic model has been further extended. An improved Bouc-Wen model with degradation was proposed by Baber and Wen [58], which can be expressed as follows

$$\dot{z} = \frac{1}{\eta}\left[A\dot{u} - \rho\left(\beta|\dot{u}||z|^{n-1}z - \gamma\dot{u}|z|^n\right)\right] \tag{31}$$

where η and ρ are the degradation shape functions [59]. A simplified parameters of Eq. (31) can be written as

$$q = \left[\mathrm{q}_1 = \frac{A}{\eta}, q_2 = \frac{\rho\beta}{\eta}, q_3 = \frac{\rho\gamma}{\eta}, q_4 = n\right]^T \tag{32}$$

where parameters meet requirements of $q_1 > 0, |q_3| \leqslant q_2, q_4 \geqslant 1$.

The nonlinear SDOF system, as shown in Fig. 11, with the improved Bouc-Wen model is identified. The Kobe (1995) ground motion with peak ground acceleration of 3 g is used as the external excitation with the sampling frequency of 50 Hz for the duration of 40 s. Structural responses can be calculated by using the fourth to fifth order adaptive Runge-Kutta method. Seven parameters of this nonlinear system to be identified are stated as $\widehat{\theta} = \{K, C, \alpha, \mathrm{q}_1, q_2, q_3, q_4\}$.

The common parameters of Jaya, DE and AHJDE are defined as population sizes $NP = 200$, maximum iterations number $Max\_Iter = 400$. Algorithm-specific parameters $F = 0.8$, $CR = 0.85$ for DE, and samples size is set as 400 for AHJDE. Identified results for the nonlinear SDOF system with the improved Bouc-Wen model by Jaya, DE and AHJDE are listed in Table 6. It can be easily observed that the maximum errors are 4.3 % and 5.5 % for AHJDE, which are better than those identified by Jaya (7.6 % and 10.8 %) and DE (6.6 % and 15.2 %) under noise free case and 5 % noise case, respectively. Besides, Fig. 13 presents a good agreement between the measured response and estimated response with identified parameters, which indicates the proposed AHJDE algorithm can yield accurate estimates of structural parameters and nonlinear hysteretic parameters.

5. Experimental verifications

5.1. Experimental setup

To further verify the applicability of the proposed hybrid algorithm to structural identification, experimental tests on a five-story steel frame structure are conducted. Fig. 14 presents the diagram of experimental setup in the laboratory. The total height, length and width of the frame structure are 1750 mm, 300 and 400 mm, respectively. The geometries

Table 5
Identified results for the nonlinear SDOF system with classical Bouc-Wen model.

Parameter	True value	0 % noise			5 % noise		
		Jaya	DE	AHJDE	Jaya	DE	AHJDE
K	7200	7126.4(1.0)[a]	7129.5(0.9)	7185.4(0.2)	7418.7(3.0)	7039.0(2.2)	7169.8(0.4)
C	120	122.8(2.3)	123.8(3.1)	121.6(1.3)	125.4(4.5)	123.4(2.9)	123.8(3.1)
α	0.1	0.1(0.6)	0.1(6.3)	0.1(0.6)	0.1(7.3)	0.1(6.9)	0.1(2.6)
β	5	5.2(4.2)	5.1(1.5)	5.1(1.2)	5.2(3.7)	5.1(1.6)	5.2(4.2)
γ	5	5.4(8.9)	5.1(3.0)	5.1(2.0)	5.6(11.5)	5.5(9.6)	5.2(5.0)
n	2	2.0(1.4)	2.1(3.8)	2.1(1.4)	2.1(4.0)	2.1(4.7)	2.1(4.4)
Max error		8.9 %	6.3 %	2.0 %	11.5 %	9.6 %	5.0 %

[a] Relative errors of identified parameters are in the parentheses expressed in %.

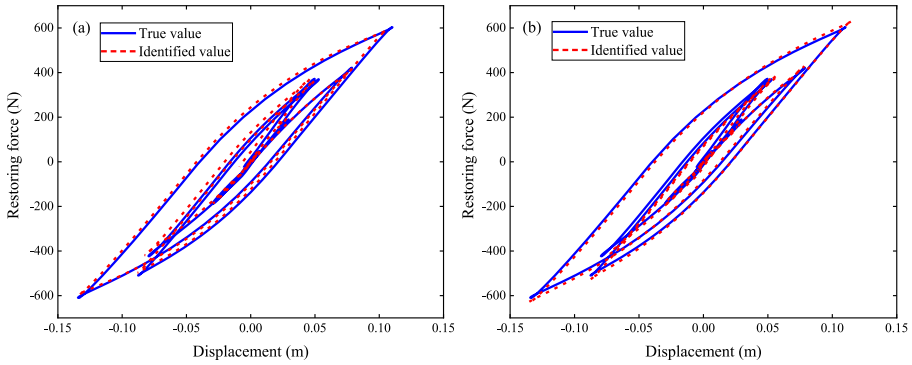

Fig. 12. The hysteretic loops of the classical Bouc-Wen model by AHJDE: (a) 0% noise; (b) 5% noise.

Table 6
Results for the nonlinear SDOF system with the improved Bouc-Wen model by Jaya, DE, AHJDE.

Parameter	True value	0 % noise			5 % noise		
		Jaya	DE	AHJDE	Jaya	DE	AHJDE
K	7200	7428.4(3.2)[a]	7036.5(2.3)	7138.6(0.9)	7548.7(4.8)	7354.6(2.1)	7041.6(2.2)
C	120	126.2(5.2)	125.1(4.2)	123.6(3.0)	122.6(2.2)	126.0(5.0)	126.2(5.2)
α	0.1	0.1(3.8)	0.1(6.2)	0.1(1.3)	0.1(10.8)	0.1(6.3)	0.1(5.5)
q_1	1	1.0(2.8)	1.1(5.7)	1.0(3.2)	1.0(2.1)	1.2(15.2)	1.0(3.9)
q_2	2	2.2(7.6)	2.1(4.0)	2.1(4.3)	2.0(2.2)	2.1(4.3)	2.1(4.6)
q_3	2	2.1(6.9)	2.1(6.6)	2.0(2.1)	2.1(5.5)	2.1(2.9)	2.1(2.7)
q_4	2	2.0(4.7)	2.0(2.4)	2.0(1.6)	1.9(5.3)	1.9(4.8)	2.0(2.5)
Max error		7.6 %	6.6 %	4.3 %	10.8 %	15.2 %	5.5 %

[a] Relative errors of identified parameters are in the parentheses expressed in %.

for each story slab are 300 × 400 × 15 mm, and all columns have identical dimension of 350 × 40 × 4 mm. Thus, this frame model can be considered as a typical shear-type structure owing to the comparatively strong floors and weak columns. The elastic modulus and mass density of steel material are 2.06×10^{11}N/m^2 and 7850 kg/m^3, respectively. A Modal Shop 2100E11 vibration exciter is tightly fixed on counterforce wall to generate random-force time history, which is recorded by force sensor, applied at the top story in the y direction. Horizontal acceleration responses of all floors are recorded by model 991C acceleration sensors and collected by the Quantum X data acquisition system. The sampling frequency is set as 50 Hz and sampling duration is 100 s. Total mass of each floor including the accelerometers are $M_1 = 24.99$ kg, $M_2 = 24.94$ kg, $M_3 = 24.93$ kg, $M_4 = 24.75$ kg, $M_5 = 24.80$ kg.

5.2. Initial model updating

In order to reduce the adverse effect of modeling error on structural damage identification, initial model updating is implemented so that the finite element model is as close to the real structure as possible. The elemental stiffness parameters are updated with the objective of minimizing the discrepancies between the natural frequencies calculated from the numerical model and extracted from the experimental data. The measured natural frequencies of this frame structure are identified from the power spectra density of recorded accelerations in frequency domain with aid of frequency domain decomposition technique (FDD), listed in Table 7. Objective function optimized by the proposed AHJDE algorithm is defined as

$$obj\left(\widehat{\underset{K}{\theta}}\right) = \sum_{i=1}^{5} \frac{\left| w_i^c\left(\widehat{\underset{K}{\theta}}\right) - w_i^m \right|}{w_i^m} \tag{33}$$

where $\widehat{\underset{K}{\theta}}$ means element stiffness to be updated, $\widehat{\underset{K}{\theta}} = [K_1, K_2, \ldots, K_{Dim}]$; w_i^c and w_i^m stand for the natural frequencies from the analytical model and physical structure, respectively.

The analytical natural frequencies of frame structure before and after updating are presented in Table 7. It can be observed that the first five natural frequencies from the updated model have a more favorable

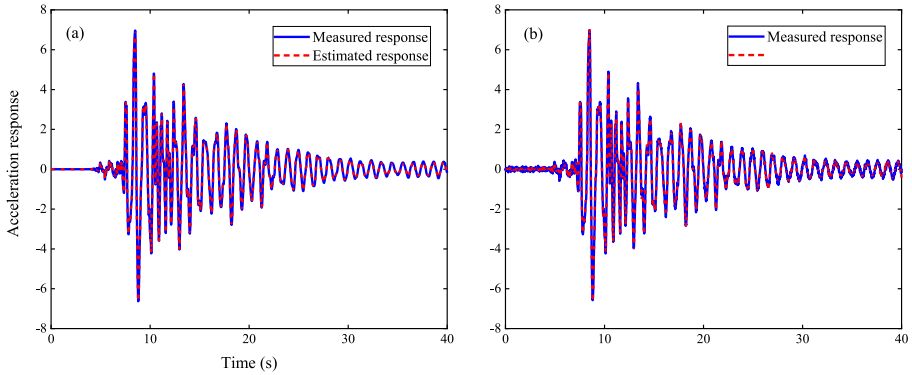

Fig. 13. The measured response and estimated response with identified parameters: (a) noise free; (b) 5% noise.

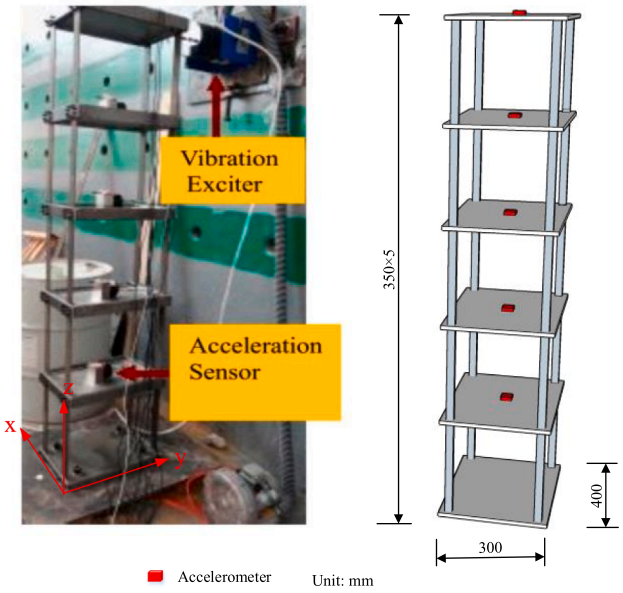

Fig. 14. Laboratory model of five-story steel frame structure.

Table 7
Measured and analytical natural frequencies of frame structure before and after updating.

Mode	Measured (HZ) (HZ)	Before updating		After updating	
		Analytical (Hz)	Relative error (%)	Analytical (Hz)	Relative error (%)
1	1.999	2.016	0.850	1.989	0.500
2	5.999	5.878	2.017	5.976	0.382
3	8.998	9.265	2.967	9.072	0.845
4	11.998	11.910	0.733	12.066	0.567
5	14.996	13.577	9.463	14.674	2.147

agreement with the measured results than those before updating. A fine initial finite element model is established considering the maximum relative error of 2.147 % for the fifth mode, which means the updated model can be taken as the baseline for the subsequent damage identification.

5.3. Damage identification results

As shown in Fig. 15, two different damage cases are investigated to test the capacity of the proposed AHJDE method for identifying damage existence, location, severity. Damages case 1 is introduced by replacing all columns in the 5th story from original width of 40 mm to smaller width of 36 mm. Similarly, damages case 2 is achieved by replacing all columns in the 4th story from initial 40 mm to more thinner columns of 32 mm. In this way, 10 % and 20 % reductions of the equivalent stiffness are introduced in the 5th and 4th floor of the steel frame structure, respectively. Fig. 16 presents the detailed reduction of cross section for damage case 1 and case 2. In fact, cutting the cross section of columns would inevitably lead to reduction of stiffness and mass parameters, which is expected to be simultaneously identified from an ideal point of view. However, less than 2 % slight reduction of mass in damage case 1 and case 2 make it difficult to be accurately identified. Thus, mass alteration is not considered in this example. AHJDE is employed to detect two damage cases with the parameter settings of population size 100, maximum generation 200, samples size 200, and the corresponding identification results are shown in Fig. 16.

By Fig. 16, it can be observed that damage location is accurately identified in most of tests, while some obvious deviations from the actual

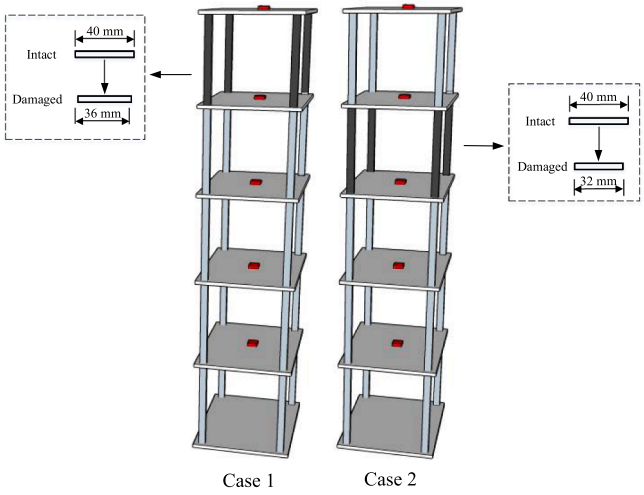

Fig. 15. Reduction of cross section in the fifth and fourth floors.

damage extent occur in the fourth test for case 1 and the first test for damage case 2, respectively. The mean values of the identified damage extent from the four tests are still satisfying considering less than 2 % and 2.5 % errors. Therefore, more reliable identification results tend to be obtained if more tests are available with the cost of increasing computational time. Fig. 17 presents the convergence history of the identified damage elements. It is noted that AHJDE takes around 30 iterations to approximately converge to the actual damage extent, namely 10 % of K_5 in cases1 and 20 % of K_4 in cases 2. These results clearly imply that the proposed hybrid method is capable of accurately and efficiently identifying damage location and extent.

6. Conclusions

An adaptive hybrid Jaya and differential evolution algorithm is proposed based on Jaya and DE to identify structural system and damages. In the proposed AHJDE, mutation pool strategy is introduced by effectively combining the powerful global exploration capacity of DE and local exploitation capacity of Jaya to generate promising candidate solutions. Besides, adaptive mutation and crossover operators, sampling-based resizing search space and linear resizing population size are integrated into the proposed algorithm. The accuracy and effectiveness of AHJDE are validated by numerical examples of a 20-DOF linear system and a nonlinear SDOF system with Bouc-Wen model, as

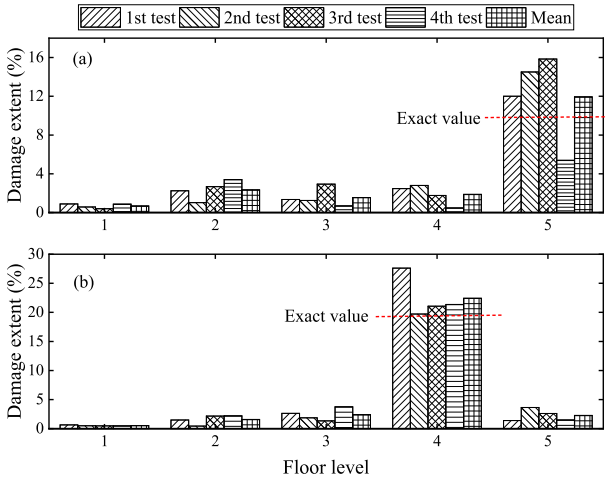

Fig. 16. Identified damage results of the frame structure: (a) damage case 1; (b) damage case 2.

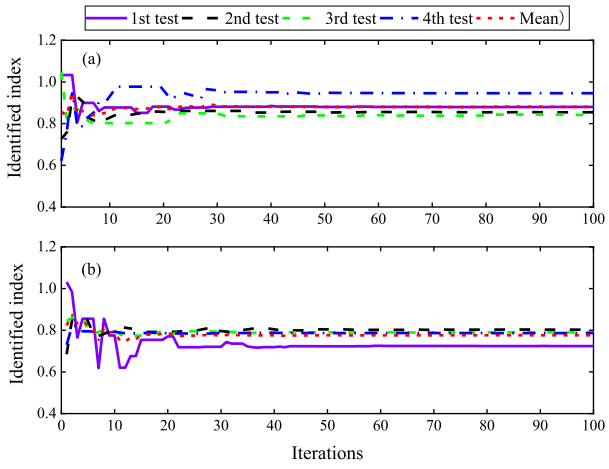

Fig. 17. The convergence histories of the damage element: (a) K_5 in case 1; (b) K_4 in case 2.

well as experimental verifications on a five-story steel frame structure. Some conclusions can be drawn as below:

(1) In the numerical studies on a 20-DOF linear system, the proposed AHJDE shows more favorable computational efficiency but presents much better accuracy in structural parameter identification than PSO, DE, SSRM, modified ABC, C-TSA, IBOA. Satisfactory identification results can be achieved for 20-DOF unknown mass system with maximum errors of 3.62 %, 4.40 %, 8.62 % in stiffness, mass, damping under 10 % noise.

(2) For the identification of a nonlinear SDOF system with classical and improved Bouc-Wen hysteretic models, favorable results prove that AHJDE can more accurately identify unknown structural parameters and nonlinear hysteresis parameters than Jaya and DE.

(3) Experimental studies on the steel frame structure demonstrate that the proposed method can obtain accurate results in the identification of the damage existence, location, severity. More reliable damage identification results could be achieved by taking the average results of multiple experiments.

(4) Reliable results in numerical and experimental studies show that the proposed AHJDE is effective, efficient, robust to identify structural systems and damages even with partial and noise-polluted measurements.

It is noted that the proposed hybrid algorithm successfully identifies parameters of 20-DOF linear system and nonlinear SDOF system, while some aspects are not considered in present paper, such as modelling error, temperature variation, boundary stiffness alternation, optimal sensor placement, which would be investigated on more complex and large-scale engineering structures in the future study.

Declaration of Competing Interest

The authors declare that they have no known competing financial interests or personal relationships that could have appeared to influence the work reported in this paper.

Acknowledgments

This research was supported by the Key Program of Intergovernmental International Scientific and Technological Innovation Cooperation (2021YFE0112200), the Japan Society for Promotion of Science (Kakenhi No. 18K04438), the Tohoku Institute of Technology research Grant. These financial supports are sincerely appreciated. Besides, the author(s) would like to thank the anonymous reviewers for their detailed and fruitful remarks.

References

[1] Doebling SW, Farrar CR, Prime MB. A summary review of vibration-based damage identification methods. Shock Vib Dig 1998;30(2):91–105.
[2] Fan W, Qiao P. Vibration-based damage identification methods: a review and comparative study. Struct Health Monit 2011;10(1):83–111.
[3] Hou RR, Xia Y. Review on the new development of vibration-based damage identification for civil engineering structures: 2010–2019. J Sound Vib 2021;491:115741.
[4] Kaveh A, Hamedani KB, Kamalinejad M. Improved slime mould algorithm with elitist strategy and its application to structural optimization with natural frequency constraints. Comput Struct 2022;264:106760.
[5] Gorgin R. Damage identification technique based on mode shape analysis of beam structures. Structures 2020;27:2300–8.
[6] Cao M, Radzieński M, Xu W, Ostachowicz W. Identification of multiple damage in beams based on robust curvature mode shapes. Mech Syst Signal Process 2014;46(2):468–80.
[7] Huang Q, Xu YL, Li JC, Su ZQ, Liu HJ. Structural damage detection of controlled building structures using frequency response functions. J Sound Vib 2012;331(15):3476–92.
[8] Huang M, Li X, Lei Y, Gu J. Structural damage identification based on modal frequency strain energy assurance criterion and flexibility using enhanced Moth-Flame optimization. Structures 2020;28:1119–36.
[9] Perry MJ, Koh CG. Output-only structural identification in time domain: numerical and experimental studies. Earthq Eng Struct Dyn 2008;37(4):517–33.
[10] Askari M, Yu Y, Zhang C, Samali B, Gu X. Real-time tracking of structural stiffness reduction with unknown inputs, using self-adaptive recursive least-square and curvature-change techniques. Int J Struct Stab Dyn 2019;19(10):1950123.
[11] Lu ZR, Wang L. An enhanced response sensitivity approach for structural damage identification: convergence and performance. Int J Numer Methods Eng 2017;111(13):1231–51.
[12] Hoseini MR, Wang XD, Zuo MJ. Estimating ultrasonic time of flight using envelope and quasi maximum likelihood method for damage detection and assessment. Measurement 2012;45(8):2072–80.
[13] Cadini F, Sbarufatti C, Corbetta M, Cancelliere F, Giglio M. Particle filtering-based adaptive training of neural networks for real-time structural damage diagnosis and prognosis. Struct Control Health Monitor 2019;26(12):e2451.
[14] Xie L, Zhou Z, Zhao L, Wan C, Tang H, Xue S. Parameter identification for structural health monitoring with extended Kalman filter considering integration and noise effect. Appl Sci-Basel 2018;8(12):2480.
[15] Li D, Wang Y. Constrained unscented Kalman filter for parameter identification of structural systems. Struct Control Health Monitor 2022;29(4):e2908.
[16] Lu Z-R, Yang D, Liu J, Wang Li. Nonlinear breathing crack identification from time-domain sensitivity analysis. Appl Math Model 2020;83:30–45.
[17] Lei Y, Xia D, Erazo K, Nagarajaiah S. A novel unscented Kalman filter for recursive state-input-system identification of nonlinear systems. Mech Syst Signal Process 2019;127:120–35.
[18] Pathirage CSN, Li J, Li L, Hao H, Liu W, Wang R. Development and application of a deep learning–based sparse autoencoder framework for structural damage identification. Struct Health Monit 2019;18(1):103–22.
[19] Ding ZH, Li J, Hao H. Structural damage identification by sparse deep belief network using uncertain and limited data. Struct Control Health Monitor 2020;27(5):e2522.
[20] Downey A, Hu C, Laflamme S. Optimal sensor placement within a hybrid dense sensor network using an adaptive genetic algorithm with learning gene pool. Struct Health Monit 2018;17(3):450–60.
[21] Wang X, Zhang J, Sun Y, et al. Stiffness identification of deteriorated PC bridges by a FEMU method based on the LM-assisted PSO-Kriging model. Structures 2022;43:374–87.
[22] Tang HS, Xue ST, Fan CX. Differential evolution strategy for structural system identification. Comput Struct 2008;86(21–22):2004–12.
[23] Sun H, Luş H, Betti R. Identification of structural models using a modified Artificial Bee Colony algorithm. Comput Struct 2013;116:59–74.
[24] Yin Z, Liu J, Luo WL, et al. An improved Big Bang-Big Crunch algorithm for structural damage detection. Struct Eng Mech 2018;68(6):735–45.
[25] Yi TH, Li HN, Wang CW. Multiaxial sensor placement optimization in structural health monitoring using distributed wolf algorithm. Struct Control Health Monitor 2016;23(4):719–34.
[26] Kaveh A, Kamalinejad M, Biabani Hamedani K, Arzani H. Quantum Teaching-Learning-Based Optimization algorithm for sizing optimization of skeletal structures with discrete variables. Structures 2021;32:1798–819.
[27] Kaveh A, Amirsoleimani P, Dadras Eslamlou A, Rahmani P. Frequency-constrained optimization of large-scale dome-shaped trusses using chaotic water strider algorithm. Structures 2021;32:1604–18.
[28] Ding Z, Li J, Hao H, Lu Z-R. Structural damage identification with uncertain modelling error and measurement noise by clustering based tree seeds algorithm. Eng Struct 2019;185:301–14.
[29] Kaveh A, Biabani Hamedani K, Milad Hosseini S, Bakhshpoori T. Optimal design of planar steel frame structures utilizing meta-heuristic optimization algorithms. Structures 2020;25:335–46.
[30] Wang XJ, Zhang GC, Wang XM, et al. Output-only structural parameter identification with evolutionary algorithms and correlation functions. Smart Mater Struct 2020;29(3):035018.
[31] Zhou H, Zhang G, Wang X, Ni P, Zhang J. Structural identification using improved butterfly optimization algorithm with adaptive sampling test and search space reduction method. Structures 2021;33:2121–39.

[32] Rao R. Jaya: A simple and new optimization algorithm for solving constrained and unconstrained optimization problems. Int J Ind Eng Comp 2016;7(1):19–34.
[33] Ding ZH, Li J, Hao H. Simultaneous identification of structural damage and nonlinear hysteresis parameters by an evolutionary algorithm-based artificial neural network. Int J Non-Linear Mech 2022;142:103970.
[34] Singh SP, Prakash T, Singh VP, Babu MG. Analytic hierarchy process based automatic generation control of multi-area interconnected power system using Jaya algorithm. Eng Appl Artif Intell 2017;60:35–44.
[35] Kaveh A, Hosseini SM, Zaerreza A. Improved Shuffled Jaya algorithm for sizing optimization of skeletal structures with discrete variables. Structures 2021;29:107–28.
[36] Kang F, Wu YR, Li JJ, et al. Dynamic parameter inverse analysis of concrete dams based on Jaya algorithm with Gaussian processes surrogate model. Adv Eng Inform 2021;49:101348.
[37] Du D-C, Vinh H-H, Trung V-D, Hong Quyen N-T, Trung N-T. Efficiency of Jaya algorithm for solving the optimization-based structural damage identification problem based on a hybrid objective function. Eng Optimiz 2018;50(8):1233–51.
[38] Rao RV, Saroj A. A self-adaptive multi-population based Jaya algorithm for engineering optimization. Swarm Evol Comput 2017;37:1–26.
[39] Yu K, Liang JJ, Qu BY, Chen Xu, Wang H. Parameters identification of photovoltaic models using an improved JAYA optimization algorithm. Energ Convers Manage 2017;150:742–53.
[40] Yildizdan G, Baykan ÖK. A novel modified bat algorithm hybridizing by differential evolution algorithm. Expert Syst Appl 2020;141:112949.
[41] Zhou HY, Zhang GC, Wang XJ, et al. A hybrid identification method on butterfly optimization and differential evolution algorithm. Smart Struct Syst 2020;26(3):345–60.
[42] Zhang GC, Wan CF, Xiong XB, et al. Output-only structural damage identification using hybrid Jaya and differential evolution algorithm with reference-free correlation functions. Measurement 2022;199:111591.
[43] Son NN, Van KienC, Anh HPH. Parameters identification of Bouc–Wen hysteresis model for piezoelectric actuators using hybrid adaptive differential evolution and Jaya algorithm. Eng Appl Artif Intell 2020;87:103317.
[44] Xiong G, Zhang J, Shi D, Zhu L, Yuan X. Optimal identification of solid oxide fuel cell parameters using a competitive hybrid differential evolution and Jaya algorithm. Int J Hydrogen Energ 2021;46(9):6720–33.
[45] Wu C, He Y. Solving the set-union knapsack problem by a novel hybrid Jaya algorithm. Soft Comput 2020;24(3):1883–902.
[46] Luu TV, Nguyen NS. Parameters extraction of solar cells using modified JAYA algorithm. Optik 2020;203:164034.
[47] Storn R, Price K. Differential evolution–a simple and efficient heuristic for global optimization over continuous spaces. J Glob Optim 1997;11(4):341–59.
[48] Wu G, Mallipeddi R, Suganthan PN, Wang R, Chen H. Differential evolution with multi-population based ensemble of mutation strategies. Inform Sci 2016;329:329–45.
[49] Giles M, Kuo FY, Sloan IH, Waterhouse BJ. Quasi-Monte Carlo for finance applications. Anziam J 2008;50:308.
[50] Altinoz OT, Yilmaz AE, Weber GW. Improvement of the gravitational search algorithm by means of low-discrepancy sobol quasi random-number sequence based initialization. Adv Electr Comput Eng 2014;14(3):55–63.
[51] Dimov I, Georgieva R, Ostromsky Tz, Zlatev Z. Advanced algorithms for multidimensional sensitivity studies of large-scale air pollution models based on Sobol sequences. Comput Math Appl 2013;65(3):338–51.
[52] Antonov IA, Saleev VM. An economic method of computing LPτ-sequences. USSR Computational Mathematics and Mathematical Physics 1979;19(1):252–6.
[53] Luo L, Hou X, Zhong J, Cai W, Ma J. Sampling-based adaptive bounding evolutionary algorithm for continuous optimization problems. Inform Sci 2017;382-383:216–33.
[54] Tanabe R, Fukunaga AS. Improving the search performance of SHADE using linear population size reduction. In: 2014 IEEE congress on evolutionary computation (CEC), IEEE, 2014, pp. 1658-1665.
[55] Perry MJ, Koh CG, Choo YS. Modified genetic algorithm strategy for structural identification. Comput Struct 2006;84(8–9):529–40.
[56] Wen YK. Method for random vibration of hysteretic systems. J Eng Mech 1976;102(2):249–63.
[57] Ma F, Zhang H, Bockstedte A, Foliente GC, Paevere P. Parameter analysis of the differential model of hysteresis. J Appl Mech 2004;71(3):342–9.
[58] Baber TT, Wen YK. Random vibration of hysteretic, degrading systems. J Eng Mech 1981;107(6):1069–87.
[59] Ma F, Ng CH, Ajavakom N. On system identification and response prediction of degrading structures. Struct Control Health Monitor 2006;13(1):347–64.